Chalcogenide Letters Vol. 22, No. 1, January 2025, p. 57 - 76

Simulated radiation shielding parameter for energy 1 keV-100 GeV of lead-free borotellurite based glass for nuclear medicine application

N. F. Rozi [a], L. Hasnimulyati [a], A. Azuraida [b,*]
[a] *Faculty of Applied Science, Universiti Teknologi MARA Cawangan Pahang, Kampus Jengka, 26400 Bandar Pusat Jengka, Pahang, Malaysia*
[b] *Department of Physics, Centre for Defence Foundation Studies, Universiti Pertahanan Nasional Malaysia, Kem Sungai Besi, 57000 Kuala Lumpur, Malaysia*

This paper studies on the theoretical ionizing radiation shielding parameter for the glass of $\{[(TeO_2)_{0.7}\ (B_2O_3)_{0.3}]_{0.7}\ [ZnO]_{0.3}\}_{1-x}\ \{CeO_2\}_x$ by using two software; WinXCOM and Phy-X software, which investigate the ability of cerium oxide. The investigation revealed that the 5CeZBTe glass sample, which included the greatest concentration of CeO_2 (0.05 mol), showed the greatest linear attenuation coefficient (LAC) and least values in Half Value Layer (HVL) and Mean Free Path (MFP). These results suggest that 5CeZBTe glass has significant potential as an alternative to traditional lead-based radiation shielding, offering a safer environment for both patients and healthcare professionals in medical settings.

(Received October 17, 2024; Accepted January 13, 2025)

Keywords: Lead-free, Tellurite, Radiation shielding properties, Cerium oxide

1. Introduction

Lead is an ordinary component in the fabrication of radiation attenuating materials. Lead is a common heavy metal use to produce high-energy photon such as gamma ray which suitable to be used as radiation shielding. This is because lead has relatively high atomic number (Z=28), the density of 11.34 g/cm^3 and it contributed to low fabrication cost. The interaction of the materials with incident gamma rays will produce a great quality of shielding. Normally, uncoated metallic lead (Pb) is used as radiation shielding in research, nuclear medicine, radiology and many more manufacturing processes [1]. However, lead-based materials are recently considered to be toxic for humans due to the lead dust which is hazardous to people's health. Worker for those encounter the lead exposures during construction of lead shielding structures were still below limit of Occupational Safety and Health Administration action level (30 μg/m^3), but the distribution of lead concentrations exposures in the air suggests that there is still a risk for overexposure. The use of lead also contributes to environmental pollution in terms of disposal issues too. Therefore, novel shielding materials are necessary to replace existing shielding materials containing lead.

Researchers have explored a variety of radiation shielding materials to protect people and environment from harmful radiation [2]. Due to atomic number and their high densities, rare-earth oxides have gained significant interest from researchers and product innovators as potential materials for high-energy photon protection. [3]. Researchers are interested in rare-earth oxides to produce the Pb-free shielding materials. It consists of 17 elements with the same chemical properties similar which are scandium (Sc), yttrium (Y) and 15 lanthanides. Although it called "rare-earth" elements, these elements are actually quite abundant and exist in many workable deposits worldwide. This work presents a glass composition made of cerium doped zinc borotellurite glass following an empirical formula $\{[(TeO_2)_{0.7}\ (B_2O_3)_{0.3}]_{0.7}\ [ZnO]_{0.3}\}_{1-x}\ \{CeO_2\}_x$ where x = 0, 0.01, 0.02, 0.03, 0.04 and, 0.05 mol. Cerium, the second element of the lanthanides group; is an iron-grey metal rare-earth elements which is soft, malleable, as well as ductile. It is extremely reactive in water. Similar to other rare-earth elements, Cerium also exists in the technologies around us. Cerium has

* Corresponding author: azuraida@upnm.edu.my
https://doi.org/10.15251/CL.2025.221.57

been used as the core for carbon electrodes of arc lamps, as a material to polish the glass surface and also work as catalytic converter in motor vehicles as it will help to reduce the carbon monoxide emissions. Radiation shielding with a higher density material will give a better effect to people's safety. By adding rare earth elements like La and Ce enhances the gamma ray blocking effectiveness of the composites of rubber matrix when using the same amount of tantalum (Ta) and specific material thickness. When it is doped with 16 mol percent Ce, the gamma ray shielding rate reaches a maximum of 38.66 percent [4]. This shows that there is potential for us to develop a Pb-free radiation shielding which will reduce the harm to humans and be environmentally friendly. Glass is also sustainable and recyclable which makes it not only favorable material for people but also gives a great contribution to climate change and the environment as it will save the usage of natural resources [5]. There is a wide variation of glasses, but the common types of glass are borate, phosphate, and tellurite which have high density, good electrical conductivity, and elastic constant. Tellurite glass is a non-crystalline solid which has high density, low melting point, low transition temperature, high nonlinear refractive index, high dielectric constant and high refractive index [5,6].

Thus, the aim of this study is to determine the theoretical ionizing radiation shielding parameters of cerium doped zinc borotellurite glass, including mass attenuation coefficient (MAC), half value layer (HVL), mean free path (MFP), linear attenuation coefficient (LAC), effective atomic number (Z_{eff}), and electron density (N_{el}). The study also compares these parameters using WinXCOM and Phy-X programs. Hence, this research can contribute to the existing body of information for future applications.

2. Methodology

The empirical formula for cerium doped zinc borotellurite glass was $\{[(TeO_2)_{0.7}\ (B_2O_3)_{0.3}]_{0.7}\ [ZnO]_{0.3}\}_{1-x}\ \{CeO_2\}_x$; and x = 0, 0.01, 0.02, 0.03, 0.04 and, 0.05 mol. The shielding parameters were calculated by Phy-X and WinXCom programmes.

2.1. Phy-X software

Phy-X software function is to calculate the parameter of radiation shielding. It provides a wide variation of parameter like LAC, MAC, HVL, MFP, electron density (N_{el}) and effective atomic number (Z_{eff}), electron density and more. In order to obtain the data of the shielding parameter from Phy-X, the user will need to key in the composition of the sample with its density. The composition can be keyed in either in the form of mole fraction or weight fraction. Users need to make sure the sum of the mole fraction is equal to 100 or 1. Next, the user will select the energies range and the parameter calculation from the option that are provided by Phy-X. After the results of the shielding parameter are obtained, the data can be downloaded to Microsoft Excel file to help the user to create the graph.

2.2. WinXCOM software

Unlike Phy-X, WinXCOM can determine the value of cross-section or attenuation coefficients on a standard grid. WinXCOM provides total attenuation coefficient and total cross-sections for coherent scattering and incoherent scattering, photoelectric absorption and pair production. In order to use the WinXCOM, users will need to identify the materials that will be keyed in which is whether it is element, compound or mixture. Then, the method of entering the additional energies also provided. Users will choose to fill in or attach a file. Next, the detail input such as sample formula, relative weight and energy range are needed to be filled. After the user fills up all the data needed, the result of mass attenuation data or cross-sectional will be shown in table form. Similar to Phy-X, users can export the data to Microsoft Excel file to obtain the graphical display. Since WinXCOM provide the value for mass attenuation coefficient, to determine the value of other parameters such as linear attenuation coefficient (LAC), mass attenuation coefficient (MAC), half value layer (HVL), mean free path (MFP), effective atomic number (Z_{eff}) and electron density (N_{el}), user need to calculate it through the theoretical calculation.

2.3. Shielding parameters calculation

Phy-X can determine LAC, HVL, MFP, electron density (N_{el}) and effective atomic number (Z_{eff}), meanwhile WinXCOM only offers mass attenuation coefficient (MAC). Thus, formula below is used to determine the LAC.

$$LAC = (MAC)\rho \tag{1}$$

where (MAC) is the mass attenuation coefficient and ρ is the sample absorption material density [7]. The density, ρ of all samples in this study was collected from our previous work [8], as indicated in Table 1.

Table 1. Chemical composition of $\{[(TeO_2)_{0.7}\ (B_2O_3)_{0.3}]_{0.7}\ [ZnO]_{0.3}\}_{1-x}\ \{CeO_2\}_x$ glass system for different dopant (CeO_2) concentration (mole fraction) and densities of the glasses.

Glass Code	CeO_2 (mol)	Glass Composition	Density (g/cm^3)
ZBTe	0.00	$[(TeO_2)_{0.7}\ (B_2O_3)_{0.3}]_{0.7}\ [ZnO]_{0.3}$	3.69
1CeZBTe	0.01	$\{[(TeO_2)_{0.7}\ (B_2O_3)_{0.3}]_{0.7}\ [ZnO]_{0.3}\}_{0.99}\ \{CeO_2\}_{0.01}$	4.60
2CeZBTe	0.02	$\{[(TeO_2)_{0.7}\ (B_2O_3)_{0.3}]_{0.7}\ [ZnO]_{0.3}\}_{0.98}\ \{CeO_2\}_{0.02}$	4.62
3CeZBTe	0.03	$\{[(TeO_2)_{0.7}\ (B_2O_3)_{0.3}]_{0.7}\ [ZnO]_{0.3}\}_{0.97}\ \{CeO_2\}_{0.03}$	4.64
4CeZBTe	0.04	$\{[(TeO_2)_{0.7}\ (B_2O_3)_{0.3}]_{0.7}\ [ZnO]_{0.3}\}_{0.96}\ \{CeO_2\}_{0.04}$	4.67
5CeZBTe	0.05	$\{[(TeO_2)_{0.7}\ (B_2O_3)_{0.3}]_{0.7}\ [ZnO]_{0.3}\}_{0.95}\ \{CeO_2\}_{0.05}$	4.69

The HVL may be simply determined once the LAC has been established [8],

$$HVL = \frac{0.693}{LAC} \tag{2}$$

Then, the values of LAC also were used in equation (3) to calculate MFP [9],

$$MFP = \frac{1}{LAC} \tag{3}$$

The value of MAC can be applied to sum-up the total atomic cross-section (ACS) [9],

$$ACS = \frac{MAC}{N_A \sum_i^n \left(\frac{w_i}{A_i}\right)} \tag{4}$$

where Avogadro's number, N_A, atomic weight of constituent element, A_i, weight fraction of element, w_i.

The ECS is expressed in this equation (5) [9],

$$ECS = \frac{1}{N_A} \sum_i^n \frac{f_i A_i}{Z_i}\ (MAC)_i \tag{5}$$

where f_i is number of atoms of an element, i is the ith element and Z_i is the atomic number of the ith element.

The parameter of Z_{eff} can be calculated using both ACS and ECS [10],

$$Z_{eff} = \frac{ACS}{ECS} \tag{6}$$

Lastly, the N_{el} can be derived from the value of MAC and ECS,

$$N_{el} = \frac{MAC}{ECS} \tag{7}$$

The difference between both theoretical values can be estimated using equation (8) [11],

$$\Delta\% = \left|\left(\frac{WinXCOM-PhyX}{WinXCOM}\right) \times 100\right| \quad (8)$$

The theoretical results include MAC, LAC, HVL, MFP, effective atomic number (Z_{eff}) and electron density (N_{el}). The comparison value of theoretical ionizing radiation shielding parameters calculated between WinXCOM and Phy-X program also will be discussed.

3. Results and discussion

3.1. Mass attenuation coefficients (MAC)

From Table 2, the values of MAC from both programs, WinXCOM and Phy-X have been obtained and it shows that data from WinXCOM and Phy-X generally showed good agreement with each other.

Table 2. The mass attenuation coefficient calculated from WinXCOM and Phy-X results for the glass samples.

Energy (MeV)	ZBTe		Δ%	1CeZBTe		Δ%
	XCOM	Phy-X		XCOM	Phy-X	
0.001	5139	5144.103	0.0993	5180	5179.827	3.3398
0.01	115.4	116.863	1.2678	117.4	117.388	0.0102
0.1	0.8282	0.8810	6.3753	0.8926	0.8930	0.0448
1	0.05895	0.05961	1.1196	0.05962	0.05962	0.0000
10	0.03022	0.03023	0.0331	0.03031	0.03031	0.0000
100	0.04432	0.04430	0.0451	0.04451	0.04450	0.0225
1000	0.05427	0.05430	0.0055	0.05452	0.05450	0.0367
10000	0.05648	0.0565	0.0354	0.05674	0.05670	0.0705
100000	0.05683	0.0568	0.0528	0.05709	0.05710	0.0175

Energy (MeV)	2CeZBTe		Δ%	3CeZBTe		Δ%
	XCOM	Phy-X		XCOM	Phy-X	
0.001	5211	5215.552	0.0874	5246	5251.276	0.1006
0.01	116.4	117.914	1.3007	116.9	118.440	1.3174
0.1	0.8497	0.9040	6.3905	0.8605	0.9150	6.3335
1	0.05895	0.05963	1.1535	0.05895	0.05964	1.1705
10	0.03038	0.03038	0.0000	0.03045	0.03046	0.0328
100	0.04471	0.04470	0.0224	0.04491	0.04490	0.0223
1000	0.05477	0.05480	0.0548	0.05501	0.05500	0.0182
10000	0.0570	0.0570	0.0000	0.05725	0.05730	0.0873
100000	0.05735	0.05730	0.0872	0.05760	0.05760	0.0000

Energy (MeV)	4CeZBTe		Δ%	5CeZBTe		Δ%
	XCOM	Phy-X		XCOM	Phy-X	
0.001	5282	5287.001	0.0947	5320	5330.388	0.1953
0.01	117.400	118.965	1.3330	117.9	119.612	1.4521
0.1	0.8713	0.9260	6.2780	0.8826	0.9390	6.3902
1	0.05895	0.05965	1.1874	0.05895	0.05971	1.2892
10	0.03053	0.03054	0.0328	0.03061	0.03065	0.1307
100	0.0451	0.0451	0.0000	0.04531	0.04540	0.1986
1000	0.05526	0.05530	0.0724	0.05552	0.05560	0.1441
10000	0.05751	0.05750	0.0174	0.05778	0.05780	0.0346
100000	0.05786	0.05790	0.0691	0.05813	0.05820	0.1204

Table 2 summarizes the MAC between both programs. The MAC values from WinXCOM and Phy-X are similar, with a deviation of less than 7%. As an example, the MAC obtained from WinXCOM for 3CeBZTe at 1 MeV is 0.05895 cm^2/g, close to 0.05964 cm^2/g, which was obtained by Phy-X. Moreover, for ZBTe at 1000 MeV, the MAC obtained is 0.05427 cm^2/g which agrees with MAC from Phy-X which is 0.05430 cm^2/g with a small difference of 0.055%.

Table 3. The mass attenuation coefficient at 0.662, 1.17 and 1.33 MeV.

Energy (MeV)	ZBTe		Δ%	1CeZBTe		Δ%
	XCOM	Phy-X		XCOM	Phy-X	
0.662	0.07333	0.07485	2.07	0.07337	0.07490	2.09
1.17	0.05426	0.05468	0.77	0.05426	0.05468	0.77
1.33	0.05079	0.051111	0.63	0.05079	0.051109	0.63

Energy (MeV)	2CeZBTe		Δ%	3CeZBTe		Δ%
	XCOM	Phy-X		XCOM	Phy-X	
0.662	0.0734	0.07495	2.11	0.07344	0.07500	2.12
1.17	0.05426	0.05468	0.77	0.05425	0.05468	0.79
1.33	0.05078	0.051107	0.64	0.05078	0.051106	0.64

Energy (MeV)	4CeZBTe		Δ%	5CeZBTe		Δ%
	XCOM	Phy-X		XCOM	Phy-X	
0.662	0.07348	0.07506	2.15	0.07351	0.07518	2.27
1.17	0.05425	0.05468	0.79	0.05425	0.05474	0.90
1.33	0.05077	0.051104	0.66	0.05077	0.051152	0.75

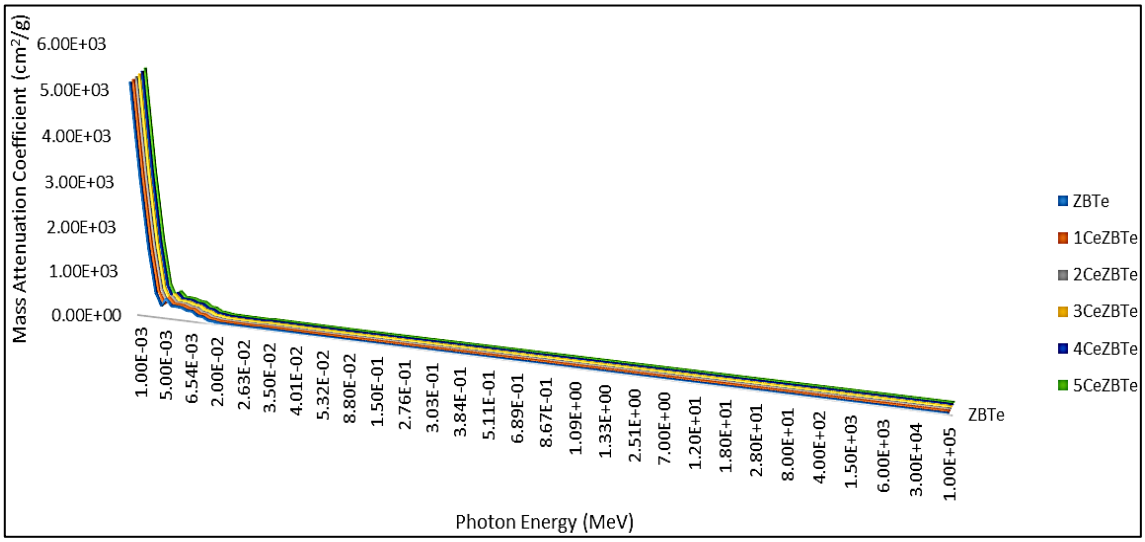

Fig. 1. The graph of MAC (cm^2/g) against photon energy (MeV) for Phy-X programs.

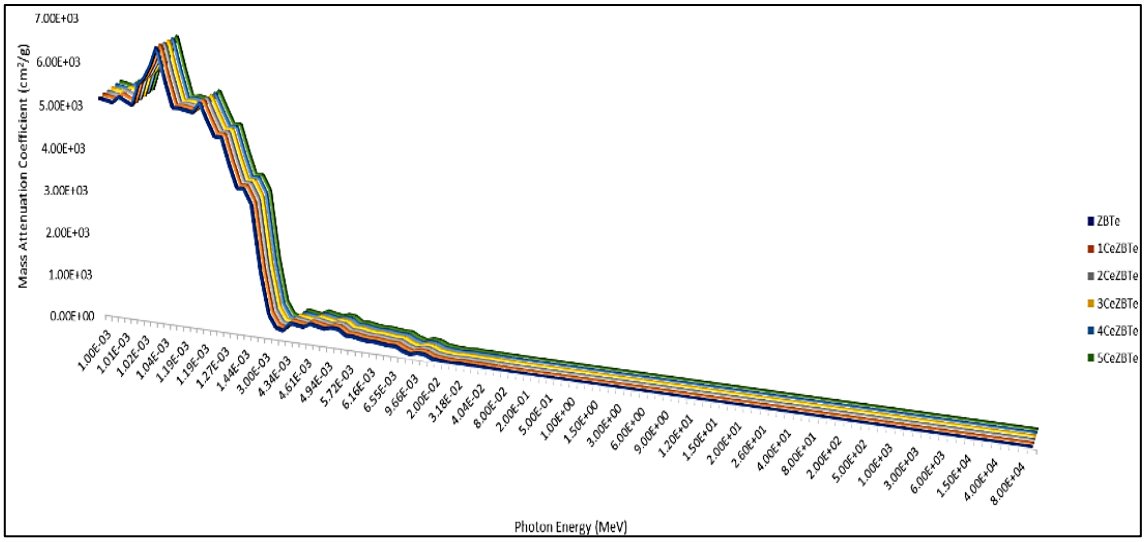

Fig. 2. The graph of MAC (cm^2/g) against photon energy (MeV) for WinXCOM programs.

The MAC values of all samples reduce drastically as the photon energy increase, but suddenly increase at the midsection. It was then slowly decreasing and became almost constant as shown in Figure 1. Meanwhile in Figure 2, the MAC values increase slowly in the low energy region but then rapidly increasing in the range 1.02×10^{-3} – 1.03×10^{-3} MeV because the photoelectric process dominates in this energy range as a result of K-absorption edge. Then, we can see that MAC rapidly decreasing in the range of energy at 0.0015 – 0.03181 MeV due to the Compton scattering. MAC became almost constant in the range 4.00×10^{-2} – 1.00×10^{5} MeV which may be due to the pair production process. It is seen that glass 5CeZBTe shows the largest MAC value in all range of energy. The mass attenuation coefficients of the chosen glasses for photon energy of 0.662, 1.17 and 1.33 MeV for cobalt-60 and cesium-137. This was done by comparing the outcomes of two different software programs. The comparison of both software is important because these energies commonly used in the industry. Cobalt-60 often used for treating cancer [12] while cesium-137 is normally utilized in low dose rate (LDR) applications. It is a by-product of nuclear reactor fission and decays through beta and gamma emissions [13]. The mass attenuation coefficients decreased with an increase in gamma-ray energies for every concentration of CeO_2. This observation is depicted in Figure 2. This suggests that large number of photon interactions happen in glass with high CeO_2 concentration and occur at low photon energy. The comparison of the mass attenuation coefficients of the glass samples calculated by WinXCON abd Phy-X was shown in Table 1 and Table 2. It also shows that there is a strong correlation between mass attenuation coefficient values.

3.2. Linear attenuation coefficient (LAC)

The linear attenuation coefficients (LAC) which obtained from two softwares (WinXCOM and Phy-X) is another important gamma-ray shielding statistic. The gamma-ray attenuation parameters of six glass samples enhanced with cerium oxide were investigated in this work (as shown in Table 4 and Table 5).

Table 4. The linear attenuation coefficient calculated from WinXCOM and Phy-X results for the glass samples.

Energy (MeV)	ZBTe		Δ%	1CeZBTe		Δ%
	XCOM	Phy-X		XCOM	Phy-X	
0.001	18962.91	18981.738	0.099	23828	23827.205	0.003
0.01	425.826	431.224	1.268	540.04	539.986	0.010
0.1	3.056	3.252	6.414	4.106	4.106	0
1	0.218	0.220	0.917	0.274	0.274	0
10	0.112	0.112	0	0.139	0.139	0
100	0.164	0.164	0	0.205	0.205	0
1000	0.200	0.200	0	0.251	0.251	0
10000	0.208	0.208	0	0.261	0.261	0
100000	0.210	0.210	0	0.263	0.263	0

Energy (MeV)	2CeZBTe		Δ%	3CeZBTe		Δ%
	XCOM	Phy-X		XCOM	Phy-X	
0.001	24236.52	24095.849	0.580	24508.48	24365.922	0.582
0.01	540.078	544.762	0.867	544.736	549.559	0.885
0.1	3.976	4.176	5.030	4.043	4.246	5.021
1	0.272	0.275	1.103	0.274	0.277	1.095
10	0.141	0.140	0.709	0.142	0.141	0.704
100	0.207	0.207	0	0.209	0.208	0.478
1000	0.254	0.253	0.394	0.256	0.255	0.391
10000	0.264	0.263	0.379	0.267	0.266	0.375
100000	0.266	0.265	0.376	0.268	0.267	0.373

Energy (MeV)	4CeZBTe		Δ%	5CeZBTe		Δ%
	XCOM	Phy-X		XCOM	Phy-X	
0.001	24844.4	24690.295	0.620	24950.8	24999.518	0.195
0.01	550.593	555.567	0.903	552.951	560.980	1.452
0.1	4.122	4.326	4.949	4.139	4.404	6.403
1	0.275	0.279	1.455	0.276	0.280	1.449
10	0.143	0.143	0	0.144	0.144	0
100	0.212	0.211	0.472	0.213	0.213	0
1000	0.259	0.258	0.386	0.260	0.261	0.385
10000	0.270	0.269	0.370	0.271	0.271	0
100000	0.271	0.270	0.369	0.273	0.273	0

Table 5. The linear attenuation coefficient in 0.662, 1.17 and 1.33 MeV.

Energy (MeV)	ZBTe		Δ%	1CeZBTe		Δ%
	XCOM	Phy-X		XCOM	Phy-X	
0.662	0.270	0.276	2.22	0.338	0.345	2.07
1.17	0.200	0.202	1.00	0.250	0.252	0.80
1.33	0.187	0.189	1.07	0.234	0.235	0.43

Energy (MeV)	2CeZBTe		Δ%	3CeZBTe		Δ%
	XCOM	Phy-X		XCOM	Phy-X	
0.662	0.339	0.346	2.06	0.341	0.348	2.05
1.17	0.251	0.253	0.80	0.252	0.254	0.79
1.33	0.235	0.236	0.43	0.236	0.237	0.42

Energy (MeV)	4CeZBTe		Δ%	5CeZBTe		Δ%
	XCOM	Phy-X		XCOM	Phy-X	
0.662	0.343	0.351	2.33	0.345	0.353	2.32
1.17	0.254	0.255	0.39	0.255	0.257	0.78
1.33	0.237	0.239	0.84	0.238	0.240	0.84

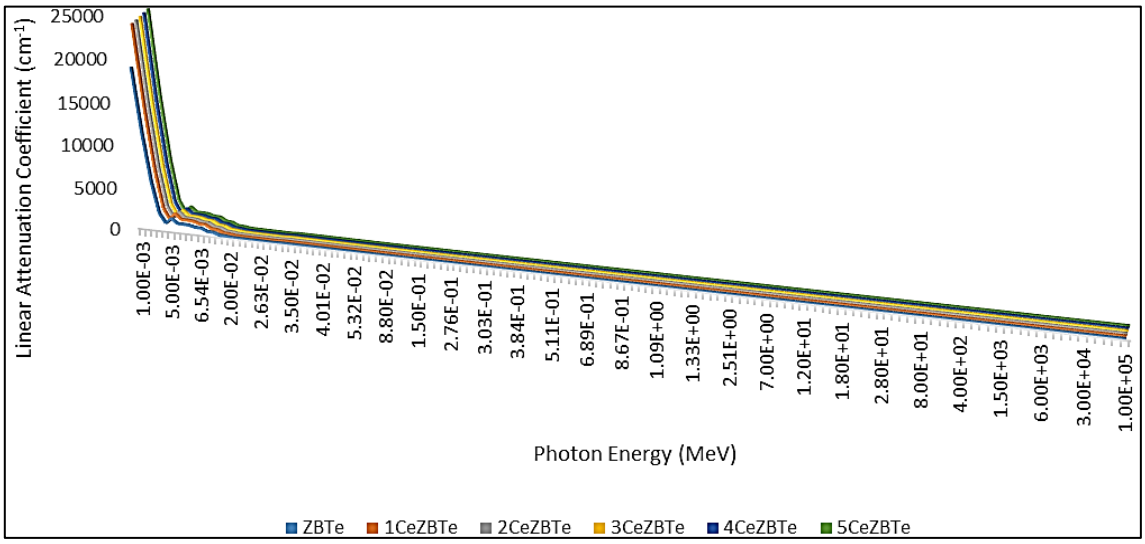

Fig. 3. The graph of linear attenuation coefficient (LAC) against photon energy (MeV) from Phy-X simulation.

It is assumed that there is a relationship between density and the linear attenuation values, and the amount of cerium oxide, since the linear attenuation coefficient depends on density. Figure 3 depicts the linear attenuation coefficients dropped to as low as 0.004 MeV as the photon energy increased. The photoelectric effect governs at the low-energy region. This is where the majority of photon–matter interactions occur. The highest linear attenuation coefficients were observed at the lowest energy region. The pair creation process dominates at 0.005 MeV, causing a slight increase in LAC values in this region. Compton scattering becomes increasingly important for medium-level energies above 0.006 MeV, considering the changes in chemical composition of the glass samples.

Since the cross section of Compton scattering is proportional to the atomic number Z. The LAC values of the glasses decreased slowly and remained stable below 0.02 MeV. No significant changes were observed in the linear attenuation coefficients as the density of the glass changed slowly. At various energies, a fascinating impact of cerium oxide on the photon resistance of glass samples has been observed. The 5CeZBTe sample that has the highest concentration of cerium oxide, exhibited the highest linear attenuation coefficients for all incident photon energies. This is caused by the 5CeZBTe sample density.

3.3. Half value layer (HVL)

Half value layer (HVL) is an additional parameter obtained from MAC values that describes the blocking capability of the materials. HVL is the thickness of a material required to reduce the incident radiation intensity by half. The lower the HVL value, the better the shielding performance against gamma rays; a material with lower HVL values may attenuate more photons. The HVL values of the selected glass system. Have been plotted against photon energy, which is shown in Figure 4. It is clear that 5CeZBTe glass has the lowest HVL values compared to 1CeZBTe glass. The 5CeZBTe glass only contains 0.01 mol percent of CeO_2 due to its high CeO_2 content. As shown in Table 4.7, at 0.662 MeV, the HVL values for 1CeZBTe and 2CeZBTe are 2.051 cm and 2.009 cm, sequentially. As in the case of transmission, the HVL values grow as the photon energy increases. As the energy of 3CeZBTe grows from 0.1 to 1 MeV, the HVL value increases from 0.171 cm to 2.53 cm. Different researches have observed that the HVL of any sample is oppositely related to the sample's density and that density has a significant effect on the HVL value. The 5CeZBTe sample has the greatest density and the lowest HVL, whereas the ZBTe sample with the least density has the highest HVL. Half value layer (HVL) decreased as the concentration of CeO_2 increased.

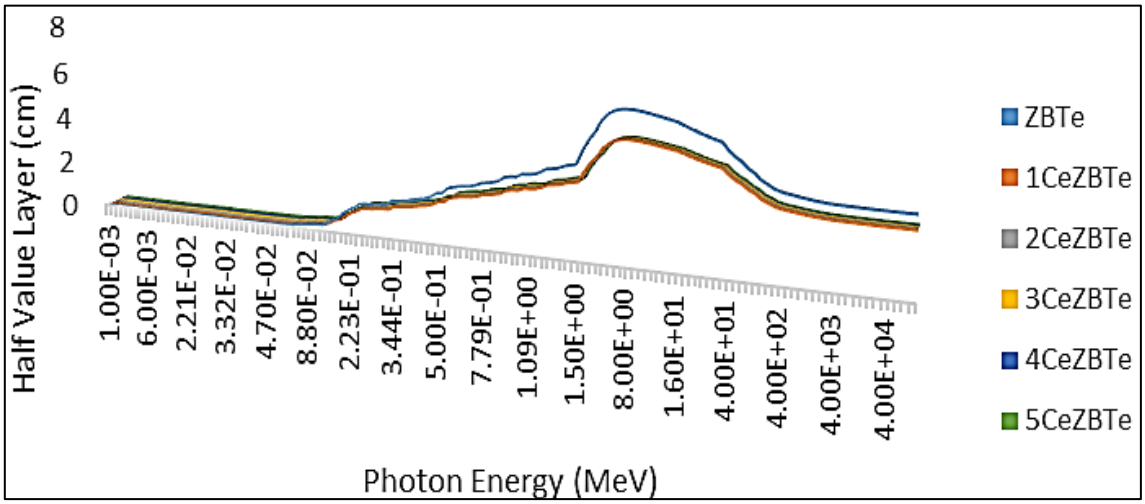

Fig. 4. The graph of half value layer against photon energy (MeV) from Phy-X simulation.

Table 6. The half value layer calculated from WinXCOM and Phy-X results for the glass samples.

Energy (MeV)	ZBTe		Δ%	1CeZBTe		Δ%
	XCOM	Phy-X		XCOM	Phy-X	
0.001	0.0000366	0.0000365	0.27	0.0000291	0.0000291	0
0.01	0.0016278	0.00161	1.09	0.0012835	0.00128	0.27
0.1	0.227	0.213	6.17	0.169	0.169	0
1	3.180	3.151	0.91	2.53	2.527	0.12
10	6.189	6.214	0.40	4.987	4.972	0.30
100	4.227	4.239	0.28	3.381	3.385	0.12
1000	3.466	3.461	0.14	2.762	2.764	0.07
10000	3.332	3.326	0.18	2.656	2.656	0
100000	3.301	3.305	0.12	2.636	2.639	0.11

Energy (MeV)	2CeZBTe		Δ%	3CeZBTe		Δ%
	XCOM	Phy-X		XCOM	Phy-X	
0.001	0.0000286	0.0000288	0.70	0.0000283	0.0000284	0.35
0.01	0.0012834	0.00127	1.04	0.0012724	0.00126	0.97
0.1	0.174	0.166	4.60	0.171	0.163	4.68
1	2.55	2.516	1.33	2.53	2.505	0.99
10	4.916	4.938	0.45	4.881	4.905	0.49
100	3.349	3.356	0.21	3.316	3.327	0.33
1000	2.729	2.740	0.40	2.708	2.716	0.30
10000	2.626	2.632	0.23	2.596	2.609	0.50
100000	2.606	2.616	0.38	2.586	2.593	0.27

Energy (MeV)	4CeZBTe		Δ%	5CeZBTe		Δ%
	XCOM	Phy-X		XCOM	Phy-X	
0.001	0.0000279	0.0000281	0.722	0.0000278	0.0000277	0.36
0.01	0.0012589	0.00125	0.71	0.0012535	0.00124	1.08
0.1	0.168	0.160	4.76	0.167	0.157	5.99
1	2.52	2.488	1.27	2.51	2.475	1.39
10	4.847	4.861	0.29	4.814	4.822	0.17
100	3.27	3.291	0.64	3.25	3.258	0.25
1000	2.676	2.686	0.37	2.666	2.659	0.26
10000	2.567	2.581	0.55	2.558	2.555	0.12
100000	2.558	2.565	0.27	2.539	2.540	0.04

Table 7. The half value layer in 0.662, 1.17 and 1.33 MeV.

Energy (MeV)	ZBTe		Δ%	1CeZBTe		Δ%
	XCOM	Phy-X		XCOM	Phy-X	
0.662	2.567	2.510	2.22	2.051	2.012	1.90
1.17	3.466	3.436	0.87	2.773	2.756	0.61
1.33	3.707	3.675	0.86	2.962	2.948	0.47

Energy (MeV)	2CeZBTe		Δ%	3CeZBTe		Δ%
	XCOM	Phy-X		XCOM	Phy-X	
0.662	2.045	2.002	2.10	2.033	1.992	2.02
1.17	2.762	2.744	0.65	2.751	2.732	0.69
1.33	2.950	2.936	0.47	2.937	2.923	0.48

Energy (MeV)	4CeZBTe		Δ%	5CeZBTe		Δ%
	XCOM	Phy-X		XCOM	Phy-X	
0.662	2.021	1.978	2.13	2.009	1.966	2.14
1.17	2.729	2.714	0.55	2.718	2.700	0.66
1.33	2.925	2.904	0.72	2.912	2.889	0.79

Energy 0.662 MeV			
Sample	HVL (cm)		Ref.
	XCOM	Phy-X	
5CeZBTe	2.009	1.966	Present work
Ordinary concrete	3.867		[14]
Hematite – serpentine	3.600		
Basalt - magnetite	2.899		
Ilmenite	2.629		
7.5 Bi_2O_3-20 CaO-10 K_2O-22.5 Na_2O-40 P_2O_5	2.480		[15]
10 Bi_2O_3-20 CaO-10 K_2O-20 Na_2O-40 P_2O_5	2.264		

Table 8. Comparison between the HVL for the tested glass with other shielding material at energy level of 0.662, 1.17 and 1.33 MeV.

Energy 1.17 MeV			
Sample	HVL (cm)		Ref.
	XCOM	Phy-X	
5CeZBTe	2.718	2.700	Present work
Ordinary concrete	5.0817		[14]
Hematite – serpentine	4.7476		
Basalt - magnetite	3.9051		
Ilmenite	3.4744		
7.5 Bi_2O_3-20 CaO-10 K_2O-22.5 Na_2O-40 P_2O_5	3.573		[15]
10 Bi_2O_3-20 CaO-10 K_2O-20 Na_2O-40 P_2O_5	3.339		
Energy 1.33 MeV			
Sample	HVL (cm)		Ref.
	XCOM	Phy-X	
5CeZBTe	2.912	2.889	Present work
Ordinary concrete	5.4194		[14]
Hematite – serpentine	5.0595		
Basalt - magnetite	4.1630		
Ilmenite	3.7086		
7.5 Bi_2O_3-20 CaO-10 K_2O-22.5 Na_2O-40 P_2O_5	3.8317		[15]
10 Bi_2O_3-20 CaO-10 K_2O-20 Na_2O-40 P_2O_5	3.5822		

In Table 8, the HVL for 5CeZBTe have been compared with different types of blocking material such as commercial glasses and concrete. Apparently, the glass sample with greatest concentration of CeO_2 have the lower value of HVLs than other types of materials. This shows that 5% cerium-doped zinc borotellurite glass is a better choice for gamma radiation shielding.

3.4. Mean free path (MFP)

MFP is the mean distance travelled by a moving particle between two consecutive collisions, where a smaller mean free path is indicated as more effective shielding material. The lower the MFP, the better the medium's radiation shielding properties. Figure 5 depicts the difference in MFP (cm) values as a function of incident photon energy. The MFP is a significant parameter in the field of radiation research, particularly for radiation shielding investigations. The MFP values of all samples used in this study were determined. The 5CeZBTe sample showed better gamma-ray attenuation and minimal MFP values at all tested photon energies.

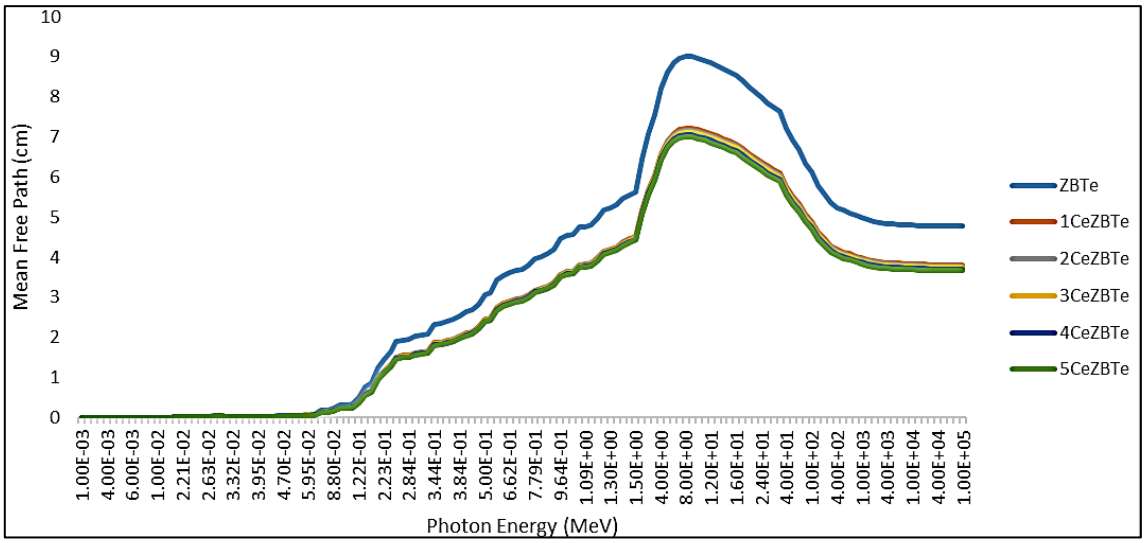

Fig. 5. The graph of mean free path against photon energy (MeV) from Phy-X simulation.

The lowest MFP value occurs at 0.001 MeV, ranging from 0.00004008 to 0.00005273 cm, while the highest MFP is at 8 MeV, ranging from 7.0029 to 9.0054 cm. Higher energy radiation penetrates material more easily, reducing the dominance of the photoelectric effect compared to the Compton interaction, which is weakly dependent on energy and atomic number. At all energies, the 5CeZBTe sample has the lowest MFP, while the ZBTe sample has the highest. For example, at 0.662 MeV, 5CeZBTe has an MFP of 2.899 cm, and ZBTe has an MFP of 3.704 cm. At 1.17 MeV, the MFPs of ZBTe and 5CeZBTe are 5.0 and 3.922 cm, respectively. These results are related to the density of the glasses, as denser materials increase photon interactions and attenuation. [16].

Table 9. Comparison of MFP between WinXCOM and Phy-X.

Energy (MeV)	ZBTe		Δ%	1CeZBTe		Δ%
	XCOM	Phy-X		XCOM	Phy-X	
0.001	0.00005273	0.00005268	0.09	0.00004197	0.00004197	0
0.01	0.0023483	0.00232	1.21	0.0018517	0.00185	0.09
0.1	0.327	0.308	5.81	0.244	0.244	0
1	4.587	4.546	0.89	3.650	3.646	0.11
10	8.929	8.965	0.40	7.194	7.173	0.29
100	6.098	6.115	0.28	4.878	4.884	0.12
1000	5.000	4.993	0.14	3.984	3.987	0.08
10000	4.808	4.798	0.21	3.831	3.831	0
100000	4.762	4.769	0.15	3.802	3.808	0.16

Energy (MeV)	2CeZBTe		Δ%	3CeZBTe		Δ%
	XCOM	Phy-X		XCOM	Phy-X	
0.001	0.00004126	0.00004150	0.58	0.00004080	0.00004104	0.59
0.01	0.0018516	0.00184	0.63	0.0018358	0.00182	0.86
0.1	0.252	0.239	5.16	0.247	0.236	4.45
1	3.676	3.630	1.25	3.650	3.614	0.99
10	7.092	7.124	0.45	7.042	7.076	0.48
100	4.831	4.841	0.21	4.785	4.799	0.29
1000	3.937	3.952	0.38	3.906	3.918	0.31
10000	3.788	3.798	0.26	3.745	3.764	0.51
100000	3.759	3.774	0.40	3.731	3.741	0.27

Energy (MeV)	4CeZBTe		Δ%	5CeZBTe		Δ%
	XCOM	Phy-X		XCOM	Phy-X	
0.001	0.00004025	0.00004050	0.62	0.00004008	0.00004000	0.20
0.01	0.0018162	0.00180	0.89	0.0018085	0.00178	1.58
0.1	0.243	0.231	4.94	0.242	0.227	6.20
1	3.636	3.590	1.27	3.623	3.571	1.44
10	6.993	7.013	0.29	6.944	6.957	0.19
100	4.717	4.748	0.66	4.695	4.701	0.13
1000	3.861	3.875	0.36	3.846	3.837	0.23
10000	3.704	3.723	0.51	3.690	3.686	0.11
100000	3.690	3.701	0.30	3.663	3.664	0.03

Table 10. The mean free path in 0.662, 1.17 and 1.33 MeV.

Energy (MeV)	ZBTe		Δ%	1CeZBTe		Δ%
	XCOM	Phy-X		XCOM	Phy-X	
0.662	3.704	3.621	2.24	2.959	2.902	1.93
1.17	5.000	4.957	0.86	4.000	3.976	0.60
1.33	5.348	5.302	0.86	4.274	4.253	0.49

Energy (MeV)	2CeZBTe		Δ%	3CeZBTe		Δ%
	XCOM	Phy-X		XCOM	Phy-X	
0.662	2.95	2.888	2.10	2.933	2.873	2.05
1.17	3.984	3.959	0.63	3.968	3.941	0.68
1.33	4.255	4.235	0.47	4.237	4.217	0.47

Energy (MeV)	4CeZBTe		Δ%	5CeZBTe		Δ%
	XCOM	Phy-X		XCOM	Phy-X	
0.662	2.915	2.853	2.13	2.899	2.836	2.17
1.17	3.937	3.916	0.53	3.922	3.895	0.69
1.33	4.219	4.190	0.69	4.202	4.168	0.81

Table 11. Comparison between the MFP for the tested glass with other shielding material energy level of 0.662, 1.17 and 1.33 MeV.

Energy 0.662 MeV			
Sample	MFP (cm)		Ref.
	XCOM	Phy-X	
5CeZBTe	2.899	2.836	Present work
Ordinary concrete	5.5803		[14]
Hematite – serpentine	5.1948		
Basalt - magnetite	4.2753		
Ilmenite	3.7950		
7.5 Bi_2O_3-20 CaO-10 K_2O-22.5 Na_2O-40 P_2O_5	3.5778		[15]
10 Bi_2O_3-20 CaO-10 K_2O-20 Na_2O-40 P_2O_5	3.2669		

Energy 1.17 MeV			
Sample	MFP (cm)		Ref.
	XCOM	Phy-X	
5CeZBTe	3.922	3.895	Present work
Ordinary concrete	7.3314		[14]
Hematite – serpentine	6.8493		
Basalt - magnetite	5.6338		
Ilmenite	5.0125		
7.5 Bi_2O_3-20 CaO-10 K_2O-22.5 Na_2O-40 P_2O_5	5.154		[15]
10 Bi_2O_3-20 CaO-10 K_2O-20 Na_2O-40 P_2O_5	4.818		

Energy 1.33 MeV			
Sample	MFP (cm)		Ref.
	XCOM	Phy-X	
5CeZBTe	4.202	4.168	Present work
Ordinary concrete	7.8186		[14]
Hematite – serpentine	7.2993		
Basalt - magnetite	6.0060		
Ilmenite	5.3504		
7.5 Bi_2O_3-20 CaO-10 K_2O-22.5 Na_2O-40 P_2O_5	5.5279		[15]
10 Bi_2O_3-20 CaO-10 K_2O-20 Na_2O-40 P_2O_5	5.1680		

In Table 11, the MFP for 5CeZBTe have been compared with different types of blocking material such as concrete and commercial glasses. Apparently, the glass sample with highest concentration of CeO_2 have the lowest value of MFP than other types of materials. Thus, it shows that 5% cerium doped zinc borotellurite glass is a better choice as gamma radiation shielding.

3.5. Effective atomic number (Z_{eff})

Effective atomic number is other important parameter for shielding analysis of materials. Z_{eff} give information about shielding material. The Z_{eff} values of material depend on both the atomic and electronic cross-section. The higher of Z_{eff} for any absorbing material means the more amount of photon energy absorbed by the material. 5CeZBTe was observed to have the maximum effective atomic number values at all energies examined, as illustrated in Figure 6. This can be explained by the increased amount of cerium oxide reinforcement, which increased the glasses' overall atomic number from ZBTe to 5CeZBTe. As a result, the 5CeZBTe sample's total atomic number changed significantly due to the increment of CeO_2 contents. The results reveal that the 5CeZBTe sample had the highest Z_{eff} values over the whole range of gamma-ray energy.

Figure 6 demonstrates the effective atomic number (Z_{eff}) of the present glasses. The lowest Z_{eff} value occurs at the energy of 1.275 MeV, and lies within the range of 14.53 – 14.84, while the greatest Z_{eff} can be found at 0.03218 MeV, within the range of 45.36 – 45.56. As energy further increases, the Z_{eff} values remain almost constant between 300 and 40000 MeV. At all energies, the Z_{eff} values are in between 14.53 and 45.56, which makes sense since the lowest atomic number within the composition is 5 for B and the highest is 58 for Ce.

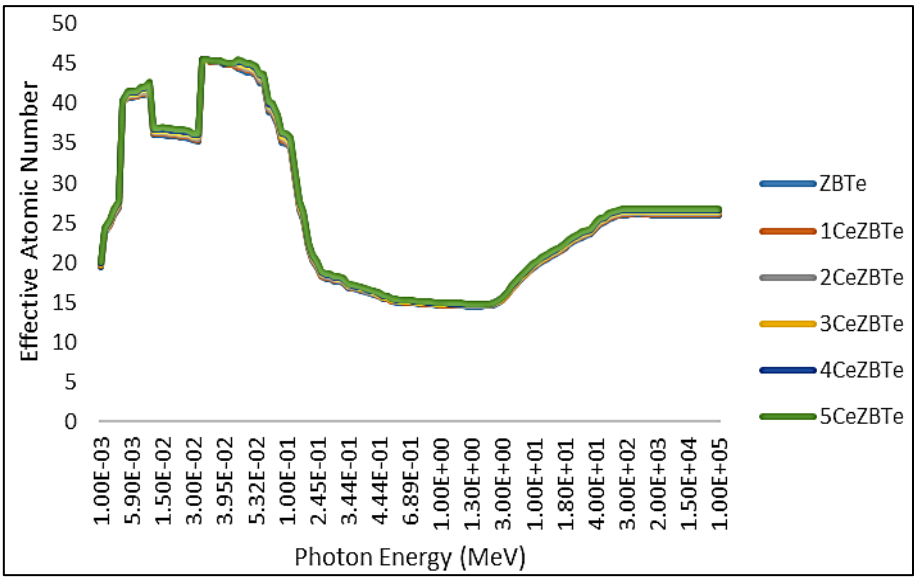

Fig. 6. The graph of effective atomic number against photon energy from Phy-X simulation.

Table 12. Comparison of Z_{eff} between WinXCOM and Phy-X.

Energy (MeV)	ZBTe		Δ%	1CeZBTe		Δ%
	XCOM	Phy-X		XCOM	Phy-X	
0.001	19.3469	19.3900	0.22	19.5575	19.5395	0.09
0.01	35.5252	36.0190	1.39	36.3151	36.2036	0.31
0.1	32.7762	34.9249	6.56	35.2460	35.1950	0.14
1	14.4270	14.6180	1.32	14.6991	14.6809	0.12
10	19.3096	19.3354	0.13	19.4746	19.4430	0.16
100	25.6344	25.6201	0.06	25.8002	25.7713	0.11
1000	25.9826	26.0152	0.13	26.1992	26.1686	0.12
10000	25.9341	25.9639	0.11	26.1479	26.1172	0.12
100000	25.9159	25.9487	0.13	26.1291	26.1019	0.10

Energy (MeV)	2CeZBTe		Δ%	3CeZBTe		Δ%
	XCOM	Phy-X		XCOM	Phy-X	
0.001	19.6444	19.6892	0.23	19.7875	19.8391	0.26
0.01	35.9076	36.3885	1.34	36.0446	36.5736	1.47
0.1	33.3341	35.4624	6.38	33.5424	35.7273	6.51
1	14.5722	14.7444	1.18	14.6219	14.8084	1.28
10	19.5594	19.5512	0.04	19.6136	19.6600	0.24
100	25.9185	25.9230	0.02	26.0413	26.0752	0.13
1000	26.3194	26.3224	0.01	26.4367	26.4766	0.15
10000	26.2666	26.2709	0.02	26.5077	26.4251	0.31
100000	26.2479	26.2556	0.03	26.4875	26.4096	0.29

Energy (MeV)	4CeZBTe		Δ%	5CeZBTe		Δ%
	XCOM	Phy-X		XCOM	Phy-X	
0.001	19.9364	19.9892	0.26	20.1065	20.1499	0.22
0.01	36.2987	36.7589	1.27	36.4112	36.9538	1.49
0.1	33.8729	35.9895	6.25	34.0759	36.2617	6.41
1	14.6964	14.8730	1.20	14.7580	14.9434	1.26
10	19.7663	19.7696	0.02	19.8644	19.8881	0.12
100	26.2447	26.2278	0.06	26.3613	26.3915	0.11
1000	26.6486	26.6312	0.07	26.7656	26.7970	0.12
10000	26.5980	26.5796	0.07	26.7159	26.7454	0.11
100000	26.5772	26.5641	0.05	26.6938	26.7297	0.13

Table 13. The Z_{eff} in 0.662, 1.17 and 1.33 MeV.

Energy (MeV)	ZBTe		Δ%	1CeZBTe		Δ%
	XCOM	Phy-X		XCOM	Phy-X	
0.662	14.7701	14.9735	0.47	14.8697	15.0438	1.17
1.17	14.4502	14.5470	0.42	14.5421	14.6086	0.46
1.33	14.4426	14.5264	0.42	14.5338	14.5872	0.37

Energy (MeV)	2CeZBTe		Δ%	3CeZBTe		Δ%
	XCOM	Phy-X		XCOM	Phy-X	
0.662	14.9174	15.1145	1.32	14.9689	15.1859	1.45
1.17	14.5851	14.6706	0.59	14.6273	14.7332	0.72
1.33	14.5747	14.6486	0.51	14.6197	14.7105	0.62

Energy (MeV)	4CeZBTe		Δ%	5CeZBTe		Δ%
	XCOM	Phy-X		XCOM	Phy-X	
0.662	15.0693	15.2578	1.25	15.1186	15.3360	1.44
1.17	14.7191	14.7963	0.52	14.7653	14.8652	0.68
1.33	14.7093	14.7729	0.43	14.7549	14.8411	0.58

3.6. Electron density (N_{el})

The electron density (Nel), representing the number of electrons per unit mass, was evaluated for the glasses. High electron density improves radiation shielding by increasing energy transfer and deposition interactions. Changes in N_{el} values are shown in Tables 14 and 15. At low photon energy, N_{el} varied non-monotonically until a sudden jump at 0.03218 MeV, due to the photoelectric process. From 0.0595 to 1.5 MeV, N_{el} values quickly decreased in all samples, related to the Compton scattering process. Above 2 MeV, N_{el} values increased due to the pair production process. The 5CeZBTe sample, with the highest cerium oxide concentration, showed a significant advantage in gamma-ray attenuation.

Table 14. Comparison of N_{el} between WinXCOM and Phy-X.

Energy (MeV)	ZBTe		Δ%	1CeZBTe		Δ%
	XCOM	Phy-X		XCOM	Phy-X	
0.001	3.6921E+23	3.6974E+23	0.14	3.7087E+23	3.7098E+23	0.03
0.01	6.7795E+23	6.8684E+23	1.31	6.8864E+23	6.8737E+23	0.18
0.1	6.2548E+23	6.6597E+23	6.47	6.6836E+23	6.6822E+23	0.02
1	2.7531E+23	2.7875E+23	1.25	2.7874E+23	2.7874E+23	0.00
10	3.6849E+23	3.6870E+23	0.06	3.6929E+23	3.6915E+23	0.04
100	4.8920E+23	4.8854E+23	0.13	4.8925E+23	4.8930E+23	0.01
1000	4.9584E+23	4.9608E+23	0.05	4.9681E+23	4.9684E+23	0.01
10000	4.9492E+23	4.9510E+23	0.04	4.9585E+23	4.9587E+23	0.00
100000	4.9456E+23	4.9481E+23	0.05	4.9549E+23	4.9558E+23	0.02
Energy (MeV)	2CeZBTe		Δ%	3CeZBTe		Δ%
	XCOM	Phy-X		XCOM	Phy-X	
0.001	3.7134E+23	3.7220E+23	0.23	3.7285E+23	3.7339E+23	0.14
0.01	6.7876E+23	6.8788E+23	1.34	6.7918E+23	6.8836E+23	1.35
0.1	6.3011E+23	6.7037E+23	6.39	6.3202E+23	6.7243E+23	6.39
1	2.7545E+23	2.7872E+23	1.19	2.7552E+23	2.7871E+23	1.16
10	3.6972E+23	3.6959E+23	0.04	3.6957E+23	3.7002E+23	0.12
100	4.8992E+23	4.9004E+23	0.02	4.9069E+23	4.9077E+23	0.02
1000	4.9750E+23	4.9759E+23	0.02	4.9814E+23	4.9832E+23	0.04
10000	4.9652E+23	4.9662E+23	0.02	4.9722E+23	4.9735E+23	0.03
100000	4.9615E+23	4.9633E+23	0.04	4.9685E+23	4.9706E+23	0.04

Energy (MeV)	4CeZBTe		Δ%	5CeZBTe		Δ%
	XCOM	Phy-X		XCOM	Phy-X	
0.001	3.7326E+23	3.7457E+23	0.03	3.7523E+23	3.7615E+23	0.25
0.01	6.7959E+23	6.8881E+23	1.29	6.7950E+23	6.8983E+23	1.52
0.1	6.3418E+23	6.7439E+23	6.03	6.3592E+23	6.7691E+23	6.44
1	2.7515E+23	2.7870E+23	1.30	2.7542E+23	2.7895E+23	1.28
10	3.7007E+23	3.7045E+23	0.01	3.7072E+23	3.7126E+23	0.15
100	4.9134E+23	4.9147E+23	0.12	4.9196E+23	4.9266E+23	0.14
1000	4.9892E+23	4.9903E+23	0.12	4.9951E+23	5.0023E+23	0.15
10000	4.9797E+23	4.9807E+23	0.12	4.9858E+23	4.9927E+23	0.14
100000	4.9759E+23	4.9777E+23	0.11	4.9816E+23	4.9898E+23	0.17

Table 15. The N_{el} in 0.662, 1.17 and 1.33 MeV.

Energy (MeV)	ZBTe		Δ%	1CeZBTe		Δ%
	XCOM	Phy-X		XCOM	Phy-X	
0.662	2.8187E+23	2.8553E+23	1.30	2.8198E+23	2.8562E+23	1.29
1.17	2.7576E+23	2.7739E+23	0.59	2.7576E+23	2.7736E+23	0.58
1.33	2.7561E+23	2.7700E+23	0.50	2.7561E+23	2.7696E+23	0.49

Energy (MeV)	2CeZBTe		Δ%	3CeZBTe		Δ%
	XCOM	Phy-X		XCOM	Phy-X	
0.662	2.8198E+23	2.7691E+23	1.33	2.8205E+23	2.8582E+23	1.34
1.17	2.7570E+23	2.7691E+23	0.59	2.7562E+23	2.7730E+23	0.61
1.33	2.7550E+23	2.7691E+23	0.51	2.7547E+23	2.7687E+23	0.51

Energy (MeV)	4CeZBTe		Δ%	5CeZBTe		Δ%
	XCOM	Phy-X		XCOM	Phy-X	
0.662	2.8591E+23	2.8591E+23	1.34	2.8628E+23	2.8628E+23	1.47
1.17	2.7726E+23	2.7726E+23	0.61	2.7749E+23	2.7749E+23	0.70
1.33	2.7682E+23	2.7682E+23	0.52	2.7705E+23	2.7705E+23	0.62

4. Conclusion

Two computer programs were used to look at how well glasses with the chemical formula $\{[(TeO_2)_{0.7}\ (B_2O_3)_{0.3}]_{0.7}\ [ZnO]_{0.3}\}1\text{-}x\ \{CeO_2\}x$ blocked gamma rays. Here, x can be 0, 0.01, 0.02, 0.03, 0.04, or 0.05 mol. Several significant radiation shielding parameters were evaluated. The glass density increased from 3.69 to 4.69 g/cm³ with increasing CeO_2 content from 0 to 0.05 mol. The 5CeZBTe glass sample, which had 0.05 mol of CeO_2, had the highest linear (LAC) and mass (MAC) attenuation coefficients for all photon energies.

The ZBTe glass sample, which did not have any CeO_2, had the lowest values. All glasses exhibited a similar trend in the half-value layer (HVL) and mean free path (MFP). ZBT > 1CeZBTe > 2CeZBTe > 3CeZBTe > 4CeZBTe > 5CeZBTe. The 5CeZBTe sample had the highest effective atomic number (Zeff) and electron density (N_{el}) values across the gamma-ray energy range. The simulation results show that the 5CeZBTe sample is better at blocking gamma rays because it has a lot of cerium oxide in it. Advanced simulations like Phy-X can be used for initial assessments of candidate glass shields to determine their gamma-ray attenuation properties before manufacture, as the difference with WinXCOM is small. The study showed that both results were in good harmony in terms of their quantitative values.

Acknowledgements

The authors appreciate the financial support for the work Universiti Pertahanan Nasional Malaysia under grant no. SF0123-UPNM/2022/SF/SG/1.

References

[1] A. H. E. Abdelhamed, K. Chan, B. W. Au, G. S. W. Thien, P. Low, Y. Sin, C. Lee, W. L. Pang, Journal of Advanced Research in Applied Sciences and Engineering Technology, 31 (2), 71(2023); https://doi.org/10.37934/araset.31.2.7180

[2] S. H. Farhan, B. M. Al Dabbagh, H. Aboud, Chalcogenide Letters, 21(6), 459 (2024); https://doi.org/10.15251/CL.2024.216.459

[3] V. P. Singh, N. M. Badiger, J. Kaewkhao, Journal of Non-Crystalline Solids, 404, 167(2014); https://doi.org/10.1016/j.jnoncrysol.2014.08.003

[4] K. Saenboonruang, W. Poltabtim, A. Thumwong, T. Pianpanit, C. Rattanapongs, Polymers, 13(12), 1930 (2021); https://doi.org/10.3390/polym13121930

[5] M. Fan, X. Ren, F. Zhou, Y. Zeng, IOP Conference Series: Earth and Environmental Science, 859(1), 012093(2021); https://doi.org/10.1088/1755-1315/859/1/012093

[6] P. Wang, S. Jia, X. Lu, Y. Jiang, J. Yu, X. Wang, S. Wang, E. Lewis, In Advanced Functional Materials. 91338(2020); https://doi.org/10.5772/intechopen.91338

[7] G. Almisned, W. Elshami, S. A. M. Issa, G. Susoy, H. M. H. Zakaly, M. Algethami, Y. S. Rammah, A. Ene, S. A. Al-Ghamdi, A. A. Ibraheem, & H. O. Tekin, Materials, 14(24). (2021); https://doi.org/10.3390/ma14247703

[8] L. Hasnimulyati, Effect Of Gamma Radiation On Elastic And Optical Properties Of Tm2o3/Ceo2-Doped Zinc Borotellurite Glass, Universiti Putra Malaysia; 281(2017).

[9] D. Cao, G. Yang, M. Bourham, D. Moneghan, Nuclear Engineering and Technology, 52(11), 2613(2020); https://doi.org/10.1016/j.net.2020.04.026

[10] A. Azuraida, M. K. Halimah, M. Ishak, N. R. Fadhilah, A. Norhayati, N. Ahmad, Chalcogenide Letters, 18(3). (2021).

[11] N. A. Nabilah Razali, I. Shahrim Mustafa, N. Z. Noor Azman, H. M. Kamari, I. S. Mat Hashim, N. Ahmad, N. A. Norazam, C. A. Shahira Che Asudin, Journal of Physics: Conference Series, 1083(1). (2018); https://doi.org/10.1088/1742-6596/1083/1/012005

[12] E. Kavaz, N. Ekinci, H. O. Tekin, M. I. Sayyed, B. Aygün, U. Perişanoğlu, Progress in Nuclear Energy, 115, 12(2019); https://doi.org/10.1016/j.pnucene.2019.03.029

[13] P. B. Roberts, Encyclopedia of Food Sciences and Nutrition, 3390(2003); https://doi.org/10.1016/B0-12-227055-X/00655-6

[14] C. M. Yashar, Clinical Gynecologic Oncology, 605.e3(2018); https://doi.org/10.1016/B978-0-323-40067-1.00023-1

[15] I. I. Bashter, Annals of Nuclear Energy, 24(17), 1389(1997); https://doi.org/10.1016/S0306-4549(97)00003-0

[16] D. A. Aloraini, A. H. Almuqrin, Sayyed, M. I., Al-Ghamdi, H., Kumar, A., M. Elsafi, Materials, 14(17) (2021); https://doi.org/10.3390/ma14175061

[17] R. Falihan, L. Hasnimulyati, N. A. Abdul-Manaf, W. Y. W. Yusoff, A. H. Azmi, A. Azuraida, Chalcogenide Letters, 19(10), 715(2022); https://doi.org/10.15251/CL.2022.1910.715